Damage Detection and Diagnosis for Offshore Wind Foundations

Bryan Puruncajas[1,2] [a], Yolanda Vidal[2] [b] and Christian Tutivén[1] [c]

[1]*Mechatronics Engineering, Faculty of Mechanical Engineering and Production Science (FIMCP),*
Escuela Superior Politécnica del Litoral (ESPOL), Guayaquil, Ecuador
[2]*Department of Mathematics, Control, Modeling, Identification and Applications (CoDAlab),*
Universitat Politècnica de Catalunya (UPC), 08019 Barcelona, Spain

Keywords: Structural Health Monitoring, Offshore Wind Turbine, Structural Vibration, Data-driven, Convolutional Neural Network.

Abstract: Structural health monitoring for wind turbines (WT) in remote locations, as offshore, is crucial (Presencia and Shafiee, 2018). Offshore wind farms are increasingly realized in water depths beyond 30 meters, where lattice foundations (as jacket-type) are a highly competitive substructure type (Moulas et al., 2017). In this work, a methodology for the diagnosis of structural damage in jacket-type foundations is stated by means of a small-scale structure -an experimental laboratory tower modeling an offshore-fixed jacket-type WT. In the literature, a lot of methodologies for damage detection can be found (Li et al., 2015). Among them, the vibration-based methods are one of the most prolific ones. However, they are, primarily, focused on the case of measurable input excitation and vibration response signals, with only few recent studies focused on the vibration–response–only case, the importance of which stems from the fact that in some applications the excitation cannot be imposed and often is not measurable. This work aims to contribute in this area, as the vibration excitation is given by the wind and analyzed by a convolutional neural network (CNN), with a classification accuracy result of 93 %.

1 INTRODUCTION

Wind energy is one of the best sources of fuel, as it is clean, relatively cheap and inexhaustible. In order to increase the energy produced by these means, more offshore wind farms have been installed (Selot et al., 2018). Given the location of wind turbines and the sea conditions, new problems related to inspection, maintenance and repair work arise (Zhang et al., 2016). To reduce logistics and maintenance costs, as well as to minimize turbine downtime, it is crucial that wind turbines are continuously monitored (Breteler et al., 2015). In particular, a structural health monitoring system (SHM) is needed to verify the state of the structure to guarantee its correct operation and determine whether the wind turbine needs some maintenance.

There are different types of WT foundations, see Figure 1, depending on the depth at which the WT will be installed. In general, monopiles are used in installations at depths below 15 meters, gravity foundations are preferred when depth is less than 30 meters, and jackets are the option used for greater depths, (Klijnstra et al., 2017). This work proposes a complete methodology for SHM (damage detection and classification) of a jacket-type foundation tested in a laboratory offshore-fixed wind turbine model. The only excitation of the WT is assumed to be given by wind turbulence, so the input excitation is assumed to be unknown. The proposed method is vibration–response–only and can be summarized in the following steps: (i) the wind excitation is simulated as a Gaussian white noise and the data coming from the WT is collected using a set of accelerometers; (ii) the raw data are pre-processed and converted into images using as many channels as sensors; (iii) a convolutional neural network is stated as a classifier. The damage detection strategy is applied to different types of predefined damage. The obtained results demonstrate the reliability of the proposed approach.

[a] https://orcid.org/0000-0002-2194-6853
[b] https://orcid.org/0000-0003-4964-6948
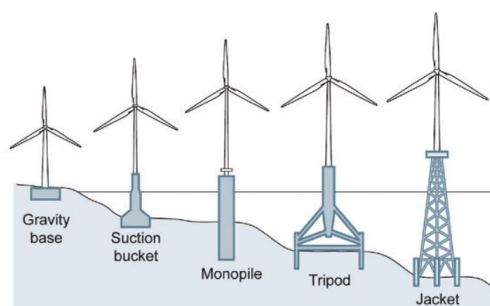[c] https://orcid.org/0000-0001-6322-4608

Figure 1: Types of foundations (Association et al., 2012).

2 RELATED WORK

The first SHM study dates back 50 years ago. In 70s and 80s, the oil industry faced the problem of identifying damage in offshore platforms (Martinez-Luengo et al., 2016). They struggled to develop methods based on identifying vibrations to locate the damage. At the same time, the aerospace community began investigating the use of vibration-based strategies. This approach has continued with the current research of the National Aeronautics and Space Administration (Seshadri et al., 2016). Currently, SHM has been developed in the fields of civil aviation industry (Khan et al., 2014) and civil structures (Song et al., 2017). SHM is highly multidisciplinary, and advances in other areas of study can probably be recruited for SHM's progress.

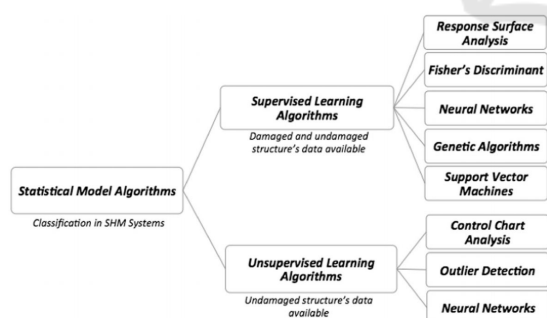Figure 2 shows a general classification for different types of strategies for SHM.

Figure 2: Algorithms classification (Martinez-Luengo et al., 2016).

The methodology implemented in this work is based on supervised learning algorithms. Specifically on neural networks (NN), which are recently used in structural health monitoring to identify, locate, and quantify damage in different types of structures (Liu et al., 2017). One of the best-known deep NNs is the convolutional neural network (CNN). A CNN is commonly used to recognize objects in images given their ability to exploit spatial or temporal correlation in the data (Albawi et al., 2017). A CNN has multiple layers; including fully connected layers, grouping layers, convolutional and nonlinear layers. Fully connected layers and convolutional layers have parameters, however non-linearity and grouping layers have no parameters.

Some research has been conducted related to CNN in the field of SHM. For example, (Tabian et al., 2019) proposes to collect impact waves using piezoelectric sensors (PZT) to detect and locate impacts (this approach was tested on a rigid panel). Another method with piezoelectric sensors is used in (De Oliveira et al., 2018), where the signals from the sensors are transformed to RGB images. A different study focused on transfer learning (TL) techniques to train with discrete histogram data (compressed data) is presented in (Azimi and Pekcan, 2019). Their results indicate that deep TL can be effectively implemented for SHM of similar structural systems with different types of sensors. However, these previous works used known-input vibration signals. In this work, it is proposed to use CNN for damage diagnosis in wind turbines foundations by using only vibration-response data. The strategy consists on transforming the vibration signals into images (with as many channels as sensors), and then classify the images with its corresponding structural state label.

3 EXPERIMENTAL SET-UP

The general overview of the experimental testbed is given in Figure 3 and explained as follows.

The experiment starts with a white noise signal given by the function generator. This signal is amplified and passed to the inertial shaker. This is responsible for generating vibrations (similar to those produced by gusts of wind on the blades) to the laboratory tower structure. The shaker is placed at the upper part of the structure, thus simulating the nacelle mass. The simulation of different wind speed is also simulated with this shaker, by changing the amplitude of the input electrical signal. In particular, multiplying it by the factors 0.5, 1, 2, and 3. Finally, the structure is monitored by 8 triaxial accelerometers which are connected to the data acquisition system. Thus, data from 24 sensors is collected. The nomenclature used for each sensor is given in Table1.

The real structure used in this work is a tower model. From Figure 3 (offshore platform) it can be seen the components of the structure: jacket, tower and nacelle. As a whole, this structure is 2.7 m high. The tower is composed of three sections joined with bolts.
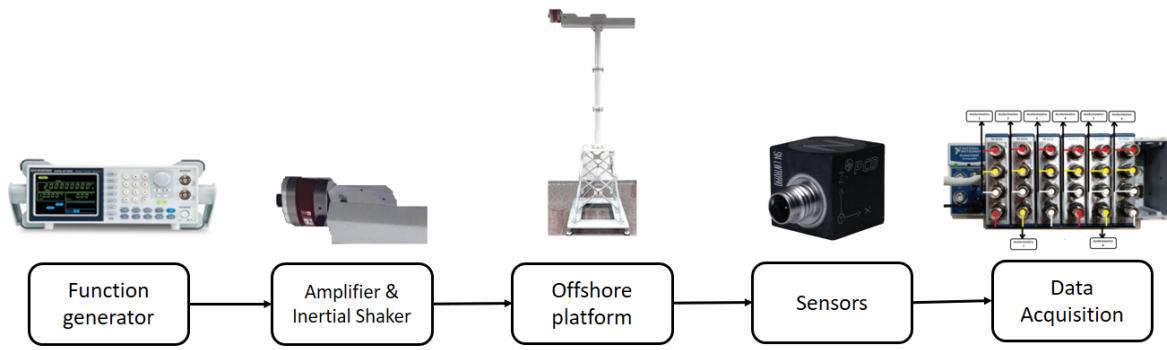
Figure 3: General overview of the experimental testbed.

Table 1: Nomenclature used to refer to each available sensor. Note that $i = 1, \ldots, 8$, as there are eight accelerometers.

	Sensor
A_i^x	Acceleration in x-direction for accelerometer number i
A_i^y	Acceleration in y-direction for accelerometer number i
A_i^z	Acceleration in z-direction for accelerometer number i

The jacket is composed with several sections, all of them joined with bolts, with a torque of 12 Nm. The different studied damages are introduced in one of these sections. The top piece (representing the nacelle) is 1 m long and 0.6 m width.

Two types of damage are introduced at the jacket support: a 5 mm crack in one of the bars; and loosening one of the bolts in the jacket. Also a healthy replica of the studied bar has been considered, as the proposed strategy should be able to detect and classify the studied types of damage, but also be robust to the replacement of one bar by a new healthy one (avoiding false alarms).

4 DAMAGE DETECTION AND CLASSIFICATION METHODOLOGY

The proposed SHM methodology is composed by the following steps. First, the data is collected from the experiment and reshaped. Second, the data is pre-processed in order to obtain a data set of multi-channel images. Third, a CNN with 24 channel inputs is designed and trained for classification of the different types of damage.

4.1 Data Collection and Reshape

The time window for each experimental test is 60 seconds with a sampling frequency of approximately 257 Hz. Thus, each experiment obtains 16517 data measurements from each of the 24 sensors. In this work,

a total of 25 experimental tests are conducted for each different white noise amplitude. In particular:

- 10 tests with the original bar.
- 5 tests with the replica bar.
- 5 tests with a 5 mm crack damaged bar.
- 5 tests with an unlocked bolt damage.

That is 100 experiments in total, as there are 25 experiments for each one of the 4 different considered white noise amplitudes. Given the k-th experimental test, the data is initially stored in a matrix $\mathbf{Y}^{(k)} \in \mathcal{M}_{16517 \times 24}(\mathbb{R})$ such that:

$$\mathbf{Y}^{(k)} = \begin{pmatrix} y_{1,1}^{(k)} & y_{1,2}^{(k)} & \cdots & y_{1,24}^{(k)} \\ y_{2,1}^{(k)} & y_{2,2}^{(k)} & \cdots & y_{2,24}^{(k)} \\ \vdots & \vdots & \ddots & \vdots \\ y_{16517,1}^{(k)} & y_{16517,2}^{(k)} & \cdots & y_{16517,24}^{(k)} \end{pmatrix}, \quad (1)$$

where the number of rows is given by the number of time stamps in each experimental test and the number of columns is equal to the number of sensors. Note that data in the first, second and third columns (A_1^x, A_1^y, A_1^z) come from accelerometer 1; fourth, fifth and sixth columns are related to the second accelerometer, and so on until the last accelerometer.

To convert the data into images, the dimensions of matrix $\mathbf{Y}^{(k)}$ have been chaned. In particular, the data coming from the k-th experimental test, $\mathbf{Y}^{(k)}$, is reshaped to a matrix $\mathbf{Z}^{(k)} \in M_{64 \times (256 \cdot 24)}(\mathbb{R})$, that is a matrix with 64 rows and $256 \cdot 24 = 6144$ columns as detailed in Table 2. Note that the last samples (from 16385 to 16517) of each sensor are discarded.

4.2 Signal to Image Conversion

The damage diagnosis method converts time-domain signals, from the 24 measured sensors, into 2D gray level images to exploit texture information from the converted images. The data conversion process is inspired in reference (Ruíz et al., 2018) but here it is enhanced by using multi-channel images.

In particular, first the values in matrix $\mathbf{Z}^{(k)}$ are scaled between 0 and 255. This will allow an easy conversion into gray scale images. The image size used for signal to image conversion is 16×16 (256 pixels) with 24 channels (one per sensor) and it is constructed as follows. For each sensor (different blocks of matrix $\mathbf{Z}^{(k)}$, see Table 2) the first 16 data-points determine the first row of the gray-scale image; immediately after, the next 16 data points determine the second row and finally the data points 240 to 256 determine the last row of the image. That is, each row of matrix $\mathbf{Z}^{(k)}$ is converted to 24 gray-scale images (one per sensor) with size 16×16. In fact, in order to apply convolutional neural networks, it is proposed to shape these data as one image with 24 channels (one per sensor), similarly to RGB images (with 3 channels). Note that, considering that the sampling time is $1/257$ seconds, each image contains approximately one second of data from all the sensors, which ensures to capture all the system dynamics. The total number of images in the data set is 6400, as there are 64 images coming from each one of the 100 experiments. Figure 4 shows one of the multi-channel images.
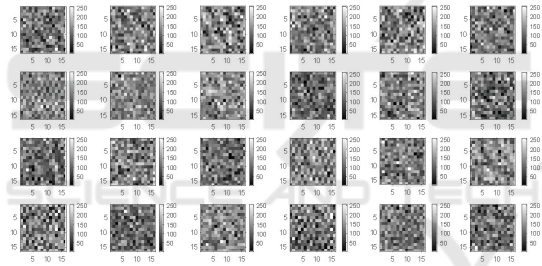

Figure 4: Multi-channel gray-scale image corresponding to the 24 sensors (size 16×16).

4.3 Convolutional Neural Network (CNN)

The next step of the proposed damage diagnosis method is to use a convolutional neural network (CNN) in order to detect and classify the damage state. The input data to the CNN are the multi-channel gray-scale images obtained from the signal-to-image

conversion explained in the previous section.

The proposed CNN architecture is shown in Figure 5 and the most significant characteristics are given in Table 3. Briefly explained, first, the gray-scale images ($16 \times 16 \times 24$) are applied to the first convolutional module. This module is composed of 32 filters (kernel 5×5) and padding of 1, resulting in an output size of $14 \times 14 \times 32$. Next, the second and the third convolutional layers have the same kernel and same padding, resulting in an output size of $12 \times 12 \times 64$ and $10 \times 10 \times 32$, respectively. Then, a fully connected layer of size $1 \times 1 \times 4$ is connected and finally, the softmax layer outputs the predicted structural condition. The data set is split into 70% for training and 30% for validation.

The parameters have been optimized with Adam, which is an adaptive learning rate method. This method is easy to implement, is computationally efficient, has few memory requirements, and hyper-parameters have intuitive interpretations and generally require little tuning (Kingma and Ba, 2014). The selected hyper-parameter values are an initial learning rate of $\alpha_0 = 0.01$, a gradient decay factor of $\beta_1 = 0.9$, a squared gradient decay factor of $\beta_2 = 0.992$, and a value $\varepsilon = 10^{-7}$. Moreover, the learning rate is drop every 2 epochs by multiplying with factor 0.5, and finally, $L2$ regularization with $\lambda = 10^{-6}$ is employed.

Finally, a flowchart of the proposed approach is shown in Figure 6. When a WT has to be diagnosed, the accelerometers data are scaled, reshaped and converted into gray-scale images that are fed into the already trained CNN. A classification is obtained to predict the condition of the structural state.

5 RESULTS

A comprehensive decomposition of the error between the true classes and the predicted classes is shown by means of the so-called confusion matrix in Table 4. Each row represents the instances in a true class while each column represents the instances in a predicted class. The first row is labeled as 1 and corresponds to

Table 2: Data reshape for each experimental test $k = 1, ..., 100$.

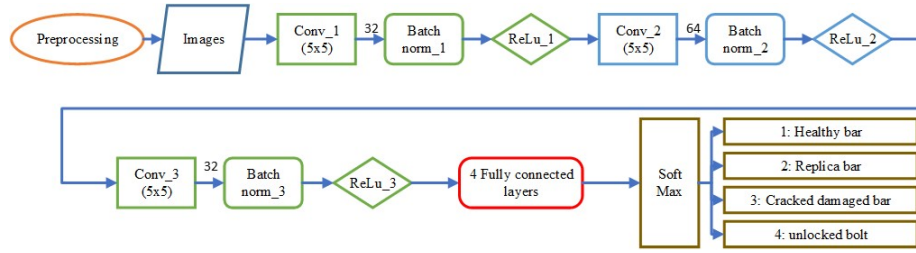|	Sensor 1		Sensor 2		. . .	Sensor 24	
$\mathbf{Z}^{(k)} =$	$\begin{bmatrix} y_{1,1}^{(k)} & \cdots & y_{256,1}^{(k)} \\ y_{257,1}^{(k)} & \cdots & y_{512,1}^{(k)} \\ \vdots & \ddots & \vdots \\ y_{16129,1}^{(k)} & \cdots & y_{16384,1}^{(k)} \end{bmatrix}$		$\begin{matrix} y_{1,2}^{(k)} & \cdots & y_{256,2}^{(k)} \\ y_{257,2}^{(k)} & \cdots & y_{512,2}^{(k)} \\ \vdots & \ddots & \vdots \\ y_{16129,2}^{(k)} & \cdots & y_{16384,2}^{(k)} \end{matrix}$		$\cdots$	$\begin{matrix} y_{1,24}^{(k)} & \cdots & y_{256,24}^{(k)} \\ y_{257,24}^{(k)} & \cdots & y_{512,24}^{(k)} \\ \vdots & \ddots & \vdots \\ y_{16129,24}^{(k)} & \cdots & y_{16384,24}^{(k)} \end{matrix}$	

Figure 5: Architecture of the developed CNN.

Table 3: Detailed characteristics of each CNN layer.

| Layer	Ouput size	Parameters
Input $16\times16\times24$ images	$16\times16\times\mathbf{24}$	-
Convolution#1 32 filters of size $5\times5\times24$ with padding [1 1 1 1]	$14\times14\times\mathbf{32}$	Weight $5\times5\times24\times32$ Bias $1\times1\times32$
Batch Normalization#1	$14\times14\times\mathbf{32}$	Offset $1\times1\times32$ Scale $1\times1\times32$
ReLu#1	$14\times14\times\mathbf{32}$	-
Convolution#2 64 filters of size $5\times5\times24$ with padding [1 1 1 1]	$12\times12\times\mathbf{64}$	Weight $5\times5\times24\times64$ Bias $1\times1\times64$
Batch Normalization#2	$12\times12\times\mathbf{64}$	Offset $1\times1\times64$ Scale $1\times1\times64$
ReLu#2	$12\times12\times\mathbf{64}$	-
Convolution#3 32 filters of size $5\times5\times24$ with padding [1 1 1 1]	$10\times10\times\mathbf{32}$	Weight $5\times5\times24\times32$ Bias $1\times1\times32$
Batch Normalization#3	$10\times10\times\mathbf{32}$	Offset $1\times1\times32$ Scale $1\times1\times32$
ReLu#3	$10\times10\times\mathbf{32}$	-
Fully connected layer#1	$1\times1\times\mathbf{4}$	Weight 4×3200 Bias 1×1
Softmax	-	-
classoutput	-	-
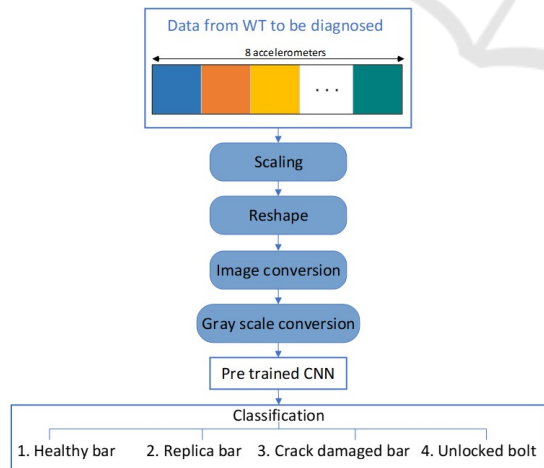
Figure 6: Flowchart to illustrate how the proposed SHM strategy is applied when a WT has to be diagnosed.

the original healthy bar, the next rows are labeled with 2, 3 and 4, corresponding to the replica bar, the crack damaged bar and the unlocked bolt, respectively.

After 64 epochs of training on a laptop running Windows 10 with an Intel Core i7-9750H, 16 GB of RAM and a graphic card (GeForce RTX 2060) of 6 GB of GPU, the obtained overall accuracy performance is 93%. A high true positive rate (TPR) of 94.04% for the original healthy bar is reached, followed by a 93.06% of TPR for the replica bar. The results for the crack damaged bar and unlocked bolt are 92.23% and 91.88% respectively. Furthermore, the obtained average recall is 92.8%, the average precision is 92.3% and, finally, a F1-score of 92.55% is achieved.

Figure 7 shows the accuracy and loss curves during the CNN training. Note that the training data set reached 100% accuracy while the validation set only obtained an accuracy of 93%. This variance could be improved with more data. However, the results confirm the viability of the proposed methodology.

5.1 Conclusions

This work proposes a SHM methodology for jacket-type wind turbine foundations using only accelerometer information. The strategy is validated experimentally for different types of predefined damages on a

Table 4: Validation set confusion matrix. The first row is labeled as 1 and corresponds to the original healthy bar, the next rows are labeled with 2, 3 and 4, corresponding to a replica bar, crack damaged bar and unlocked bolt, respectively. True positive rate (TPR) and false negative rate (FNR) of each class are given.

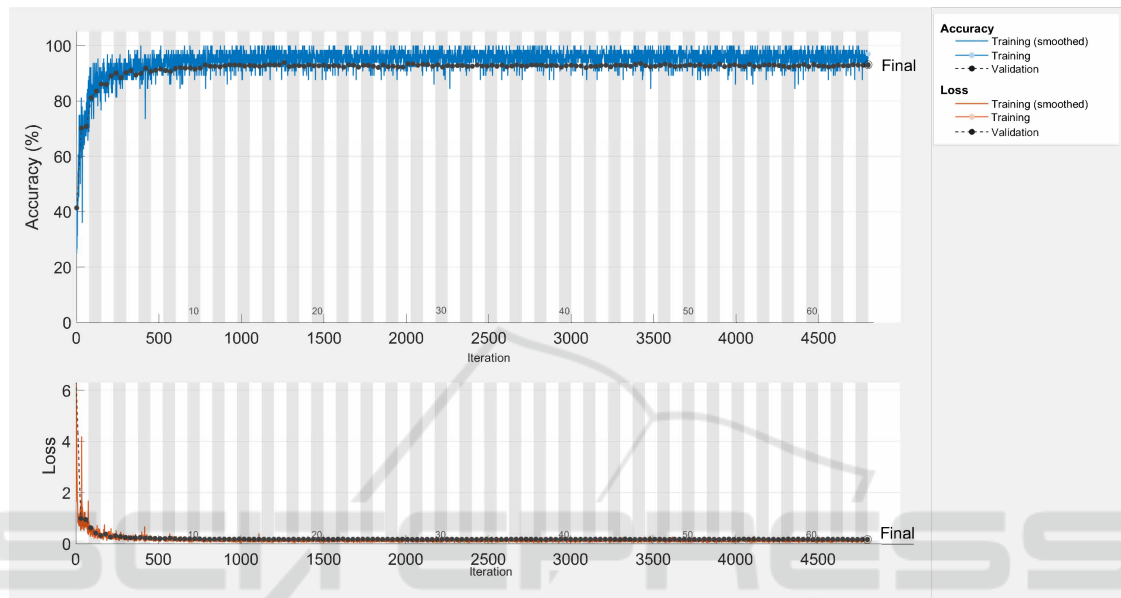|	Predicted class					TPR	FNR
	94.04	2.14	1.99	1.83	1. Healthy bar	94.04	5.96
True class	3.47	93.06	3.15	0.32	2. Replica bar	93.06	6.94
	0.65	2.91	92.23	4.21	3. Crack damaged bar	92.23	7.77
	3.75	0.63	3.75	91.88	4. Unlocked bolt	91.88	8.13

Figure 7: Accuracy and loss curves. The accuracy is represented by blue lines, the loss is represented by orange lines and the validation results are represented by black dotted lines.

small-scale laboratory tower. In a nutshell, this work applies the idea to represent time domain acceleration signals to multi-channel gray-scale images and then utilize convolutional neural networks for classification of the different structural states. The obtained results, with an overall accuracy of 93%, demonstrate the viability of the proposed approach. Future work will deal with data augmentation in order to reduce the validation error with respect to the train set error.

REFERENCES

Albawi, S., Mohammed, T. A., and Al-Zawi, S. (2017). Understanding of a convolutional neural network. In *2017 International Conference on Engineering and Technology (ICET)*, pages 1–6. IEEE.

Association, W. S. et al. (2012). Steel solutions in the green economy-wind turbines. *Brussels, Belgium*.

Azimi, M. and Pekcan, G. (2019). Structural health monitoring using extremely compressed data through deep learning. *Computer-Aided Civil and Infrastructure Engineering*.

Breteler, D., Kaidis, C., Tinga, T., and Loendersloot, R. (2015). Physics based methodology for wind turbine failure detection, diagnostics & prognostics. *EWEA 2015 Annual Event*.

De Oliveira, M. A., Monteiro, A. V., and Vieira Filho, J. (2018). A new structural health monitoring strategy based on pzt sensors and convolutional neural network. *Sensors*, 18(9):2955.

Khan, A. A., Zafar, S., Khan, N., and Mehmood, Z. (2014). History current status and challenges to structural health monitoring system aviation field. *Journal of Space Technology*, 4(1):67–74.

Kingma, D. P. and Ba, J. (2014). Adam: A method for stochastic optimization. *arXiv preprint arXiv:1412.6980*.

Klijnstra, J., Zhang, X., van der Putten, S., and Röckmann, C. (2017). Technical risks of offshore structures. In *Aquaculture Perspective of Multi-Use Sites in the Open Ocean*, pages 115–127. Springer, Cham.

Li, D., Ho, S.-C. M., Song, G., Ren, L., and Li, H. (2015). A review of damage detection methods for wind turbine blades. *Smart Materials and Structures*, 24(3):033001.

Liu, W., Wang, Z., Liu, X., Zeng, N., Liu, Y., and Alsaadi, F. E. (2017). A survey of deep neural network ar-

chitectures and their applications. *Neurocomputing*, 234:11–26.

Martinez-Luengo, M., Kolios, A., and Wang, L. (2016). Structural health monitoring of offshore wind turbines: A review through the statistical pattern recognition paradigm. *Renewable and Sustainable Energy Reviews*, 64:91–105.

Moulas, D., Shafiee, M., and Mehmanparast, A. (2017). Damage analysis of ship collisions with offshore wind turbine foundations. *Ocean Engineering*, 143:149–162.

Presencia, C. E. and Shafiee, M. (2018). Risk analysis of maintenance ship collisions with offshore wind turbines. *International Journal of Sustainable Energy*, 37(6):576–596.

Ruíz, M., Mujica, L. E., Alférez, S., Acho, L., Tutivén, C., Vidal, Y., Rodellar, J., and Pozo, F. (2018). Wind turbine fault detection and classification by means of image texture analysis. *Mechanical Systems and Signal Processing*, 107:149–167.

Selot, F., Fraile, D., and Brindley, G. (2018). Offshore wind in europe-key trends and statistics 2018.

Seshadri, B. R., Krishnamurthy, T., and Ross, R. W. (2016). Characterization of aircraft structural damage using guided wave based finite element analysis for in-flight structural health management.

Song, G., Wang, C., and Wang, B. (2017). Structural health monitoring (shm) of civil structures.

Tabian, I., Fu, H., and Sharif Khodaei, Z. (2019). A convolutional neural network for impact detection and characterization of complex composite structures. *Sensors*, 19(22):4933.

Zhang, J., Fowai, I., and Sun, K. (2016). A glance at offshore wind turbine foundation structures. *Brodogradnja: Teorija i praksa brodogradnje i pomorske tehnike*, 67(2):101–113.